Thickness dependence of the tunneling current in the coherent limit of transport

Christian Heiliger,* Peter Zahn, Bogdan Yu. Yavorsky, and Ingrid Mertig
Fachbereich Physik, Martin-Luther-Universität Halle-Wittenberg, D-06099 Halle, Germany
(Received 13 February 2008; published 4 June 2008)

We present investigations of the tunneling magnetoresistance (TMR) in planar Fe/MgO/Fe junctions performed by means of *ab initio* calculations. The electronic and magnetic structures of the junctions are calculated self-consistently in the framework of density-functional theory. The transport properties are investigated as a function of the barrier thickness in the limit of coherent tunneling. Interesting features such as sign reversal of the TMR ratio as a function of the bias voltage and of the interface structure are proven to be stable with increasing barrier thickness. It is shown that at large barrier thicknesses, only a small amount of states contributes to the overall current, but the $\mathbf{k}_{\parallel}=0$ point is not involved for all Fe/MgO/Fe junctions we considered, in contrast to the general belief supported by simplified parabolic band models. The experimentally observed saturation of the TMR ratio with increasing barrier thickness is confirmed and can be understood only analyzing the complex band structure within the whole Brillouin zone. However, we cannot confirm an oscillating behavior of the TMR ratio depending on barrier thickness as observed experimentally. This means that the measured oscillations are not an intrinsic effect of the coherent tunneling states of the ideal crystalline Fe/MgO/Fe structure.

DOI: 10.1103/PhysRevB.77.224407 PACS number(s): 75.70.Cn, 71.15.Mb, 73.63.−b, 75.30.Et

I. INTRODUCTION

Experimental investigations[1] of the thickness dependence of giant magnetoresistance (GMR) were carried out shortly after the discovery of the effect in magnetic multilayers.[2,3] Thereby, GMR and interlayer exchange coupling show similar oscillations, which can be explained by quantization effects within the nonmagnetic spacer layer.[4–6] The states causing these quantization effects can be localized on the Fermi surface of the spacer material by the so-called nesting conditions. Now one can speculate that the same behavior should be expected in tunneling magnetoresistance (TMR) measured in ferromagnet/insulator/ferromagnet sandwich structures.[7,8] Recent experimental investigations[9] show among the saturation of the TMR ratio an oscillation of the TMR ratio with increasing barrier thickness. The period of this oscillation is not equal to the atomic layer spacing. In addition, the same authors investigated the dependence of the TMR ratio on the applied bias voltage for different barrier thicknesses, but they observed almost no dependence on the barrier thickness. In general, for one particular thickness, different bias voltage dependencies are observed experimentally.[9,10] This discrepancy can be understood considering different interface structures between the Fe leads and the MgO barrier.[11–14] The role of the interface structure on tunneling was investigated in a variety of experiments[15–17] and was calculated in previous papers.[13,14] Strong changes of conductance and TMR ratio were obtained in all cases. To elucidate the appearance of features in the current-voltage characteristics, it is essential to discuss in detail the electronic states contributing to the current. Due to the fact that the features in the current-voltage characteristics are determined by a few states in the two-dimensional (2D) Brillouin zone with different exponential decay lengths in the MgO, it is not obvious that features calculated for one barrier thickness still survive for other thicknesses.

The aim of the present paper is the investigation of the transport properties as a function of barrier thickness with the help of *ab initio* calculations for different interface geometries in the coherent limit of transport. The experimentally observed saturation of the TMR ratio with increasing barrier thickness can be understood by the complex band structure of MgO and is a direct result of the electronic structure. No additional assumption such as defect scattering suggested by other authors[18,19] is necessary although such processes will strengthen the effect of saturation. For this purpose, a detailed discussion of the complex bands in the whole two-dimensional Brillouin zone is essential, which is an extension of the analysis by Butler *et al.*[11] The striking features of the current-voltage characteristics persist also for large barrier thicknesses, which can be understood by a detailed analysis of the interface electronic structure but is restricted to the systems we considered. This means that it is possible to have different current-voltage characteristics depending on the barrier thickness for other tunnel junctions or other interface geometries. It will be shown that an oscillation of the TMR ratio caused by the coherent electronic structure is not feasible since the real parts of the complex wave vectors of the contributing states inside the MgO barrier are zero.

All our calculations are focused on epitaxially grown Fe/MgO/Fe systems. Very accurate data of the interface atomic structure are available for these junctions.[9,20,21] We studied the effect of mixed Fe/O interfaces on the electronic structure and on the conductance of the Fe/MgO/Fe tunnel junction. Three types of junction geometries are discussed. All the structural data of the interface configurations are identical to our previous works.[13,14] One geometry has ideal Fe/MgO interfaces. In the second geometry both interfaces contain a mixed FeO layer. The junction remains symmetric. In our study, all oxygen sites in the interface layer are occupied and the in-plane periodicity is kept. Partial occupancy of the FeO layer by the oxygen atoms as found in experiment[20] is not discussed in this work but can change the bias dependence drastically.[22] The third configuration we considered contains both one ideal and one mixed FeO interface and will be labeled asymmetric.

 ©2008 The American Physical Society

II. METHOD

The electronic structure of the systems was calculated self-consistently within the framework of density-functional theory using a screened Korringa–Kohn–Rostoker Green's function method well suited to treat systems of dimensions comparable to experimentally investigated systems.[23,24] For the self-consistent calculations a superlattice geometry with six MgO layers sandwiched by ten Fe layers was used. Six MgO layers are sufficient to decouple both interfaces magnetically. The MgO layers in the center of the barrier have the same properties such as MgO bulk material. Therefore, the larger barrier thicknesses were built by inserting additional potentials of the central MgO layer without an extra self-consistent cycle. For the conductance calculations, a system with infinite Fe electrodes is constructed and the semi-infinite boundary conditions are taken into account explicitly. The obtained electronic and magnetic properties are in very good agreement with previous calculations.[11,12]

Due to the in-plane translational invariance, the eigenstates of the electrodes are labeled by the in-plane wave vector $\mathbf{k}_\parallel$. The transmission probability as introduced by Landauer[25] was computed using a Kubo formalism expressed in terms of the Green's function of the semi-infinite system.[26] The total transmission T at a certain energy E is obtained by a two-dimensional integration over the interface Brillouin zone and the assumption of conduction in parallel by the two spin channels,[27]

$$T(E) = \sum_\sigma \int d^2\mathbf{k}_\parallel T^\sigma_{\mathbf{k}_\parallel}(E), \tag{1}$$

with the transmission probability $T^\sigma_{\mathbf{k}_\parallel}(E) = \mathrm{Tr}[J^\sigma_L(E)G^\sigma_{LR}(\mathbf{k}_\parallel,E)J^\sigma_R(E)G^\sigma_{RL}(\mathbf{k}_\parallel,E)]$. The planes L and R are located on both sides of the barrier in the unperturbed electrode regions. $J^\sigma_{L,R}(E)$ are the current operator matrices and $G^\sigma_{LR}(\mathbf{k}_\parallel,E)$ are the Green's function elements connecting both sides of the junction.[28] The used k point meshes were at least 40 000 points in the whole Brillouin zone. For some larger barrier thicknesses, we used also denser mesh to reach better convergence if necessary.

Applying an external bias voltage V, the chemical potentials of the electrodes μ_R and $\mu_L = \mu_R + eV$ are shifted with respect to each other. Due to the small transmission, we assumed a linear voltage drop inside the MgO barrier, which was confirmed by self-consistent calculations.[12] From Ref. 12 the estimated typical charging in a tunnel junction for a bias voltage of 1 V is very small, less than 0.01 eV for 8 monolayers of MgO. With increasing barrier thickness this charging is decreasing. Therefore, we neglect these charging effects in out calculations. The current density $I(V)$ is obtained by an energy integration between μ_R and μ_L to cover all tunneling states,

$$I(V) = \frac{e^2}{h}\frac{1}{e}\int_{\mu_R}^{\mu_L} dE T(E). \tag{2}$$

The current density was calculated for parallel (P) and antiparallel (AP) alignments of the magnetic moments in the Fe electrodes. Due to the negligible magnetic interaction between the electrodes, a frozen potential approximation was applied to construct the effective potential for the AP configuration from the P configuration.[29,30]

III. COMPLEX BAND STRUCTURE IN MgO

Before we discuss the transport properties as a function of the barrier thickness, it is advantageous to recall and extend the current understanding of the origin of TMR in Fe/MgO/Fe tunnel junctions. Mavropoulos *et al.*[31] figured out the role of the complex band structure of an insulator to understand the tunneling process in a ferromagnet/insulator/ferromagnet tunnel junction. In particular, the imaginary part of the complex wave vectors and the symmetry of the states are of special importance. Twice the imaginary wave vector defines the exponential decay rate of the transmission probability with barrier thickness. The analysis of Butler *et al.*[11] of the complex band structure at the $\bar{\Gamma}$ point leads to a simple picture to understand the origin of a high TMR ratio in Fe/MgO/Fe. They found out that the complex band with the smallest imaginary wave vector has Δ_1 symmetry and the band with the second lowest imaginary wave vector is of Δ_5 symmetry. This symmetry selection of the MgO barrier is transformed into a spin filtering via the ferromagnetic Fe electrodes. Fe has Δ_1 states at the $\bar{\Gamma}$ point only in the majority spin. Therefore, electrons in this spin channel can tunnel more effectively than electrons in the minority-spin channel. This leads to a high spin polarization of the current and to a high TMR ratio. Following this idea, the TMR ratio has to increase exponentially with increasing barrier thickness due to the different decay rates at the $\bar{\Gamma}$ point. This is in contradiction to experimental results where the TMR ratio saturates for barrier thicknesses above 2 nm.[9] We show that this behavior is in agreement with the treatment of the transport in the coherent limit but it is essential to take into account contributions of the whole Brillouin zone [compare Eq. (1)]. The simple picture considering the $\bar{\Gamma}$ point only does not describe the system completely and an extension to the whole Brillouin zone is necessary to explain the experimental results.

For this purpose, the imaginary part of the wave vector of the two complex bands corresponding to the Δ_1 and Δ_5 symmetries at the $\bar{\Gamma}$ point is shown in Fig. 1 in the whole Brillouin zone. Due to their symmetry at the Brillouin-zone center, the bands are labeled Δ_1- and Δ_5-like in the following. The imaginary wave vector of the Δ_1-like states is smallest around the $\bar{\Gamma}$ point, whereas the imaginary wave vector of the Δ_5-like states is larger at the Brillouin-zone center. There are areas far away from the zone center where both states have the same decay length (green areas in Fig. 1). Based on this analysis, the symmetry selection by the barrier at the $\bar{\Gamma}$ point can be extended to an area around the Brillouin-zone center distinguishing between states coupling primarily to the Δ_1-like band and to the Δ_5-like band in MgO, respectively.

In summary, the MgO barrier performs a selection of tunneling states by providing a complex Δ_1-like and a Δ_5-like

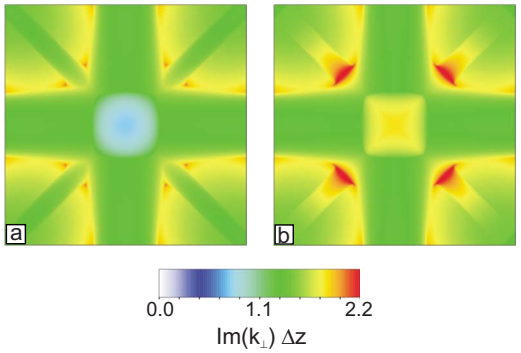

FIG. 1. (Color online) Imaginary part of the complex wave vector of MgO at the Fermi level in the 2D Brillouin zone. (a) Δ_1-like band (Δ_1 symmetry at $\bar{\Gamma}$ point). (b) Δ_5-like band (Δ_5 symmetry at $\bar{\Gamma}$ point). Δz is the MgO interlayer spacing of 0.215 nm.

band near the Brillouin-zone center. The symmetry selection is strictly valid only at the $\bar{\Gamma}$ point. At other $\mathbf{k}_\parallel$ points, the strength of the coupling is defined by the matching of metal and barrier wave functions.

IV. ZERO BIAS

We start with the discussion of our results in the zero-bias limit. For this purpose Figure 2 shows the area resistance product $RA=[(e^2/h)T(E_F)]^{-1}$ and the corresponding TMR ratio as function of the barrier thickness for all three interface geometries we considered. The calculations were done over a wide range of thicknesses between 6 and 30 monolayers of MgO. Actually, we consider a very small voltage of 13 mV to avoid possible sharp resonances for certain $\mathbf{k}_\parallel$ points at exactly 0 V. Typical experimentally investigated thicknesses are between 6 and 15 monolayers of MgO.[9] The presented TMR ratios are given by the optimistic definition where the difference of the resistance for antiparallel (AP) and parallel (P) alignments of the moments in the Fe electrodes is divided by the smaller resistance,

$$\frac{RA^{\mathrm{AP}} - RA^{\mathrm{P}}}{\min(RA^{\mathrm{P}}, RA^{\mathrm{AP}})}. \tag{3}$$

An exponential increase in the area resistance product RA depending on the barrier thickness is observed especially for

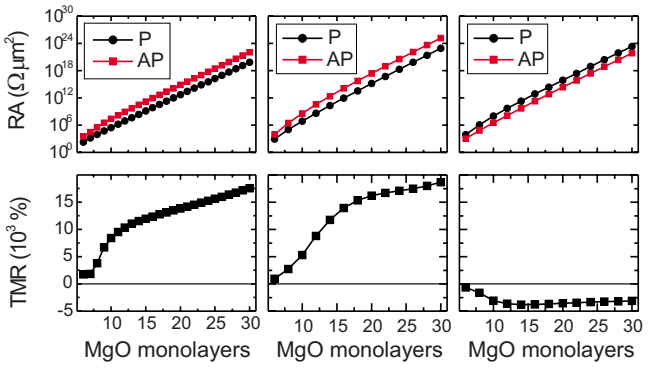

FIG. 2. (Color online) Dependence of area resistance product (top) and TMR ratio (bottom) on the barrier thickness for all geometries we considered for zero bias: left, ideal and middle, symmetric.

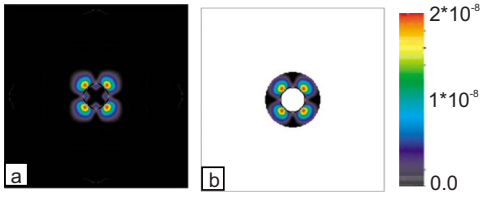

FIG. 3. (Color online) $\mathbf{k}_\parallel$-resolved total transmission for the symmetric junction in the P configuration with a barrier thickness of 10 MgO monolayers. (a) The whole Brillouin zone and b) the annulus in which the states are located which carry 90% of the total current

very large thicknesses, which demonstrates that the method is numerically stable even for very thick barriers. The slope is different for the three junctions at small barrier thicknesses. The slope is lowest for the ideal structure and slightly higher than observed in experiment.[9] The TMR ratio as a function of barrier thickness shows a quite universal behavior. A strong increase is obtained for small thicknesses and almost a saturation is reached for the symmetric and asymmetric geometries at larger thicknesses in agreement with experiments.[9] For the ideal junction the TMR is linearly increasing with the barrier thickness and not exponentially like expected using the symmetry argument at the $\bar{\Gamma}$ point only. We show in Sec. V that in the limit of very large barrier thicknesses, one expects a saturation even for the ideal junction. This means no additional assumptions such as scattering processes at defects are necessary as proposed by other authors[18] to explain the saturation. The saturation effect is, however, stronger by including additional scattering and occurs therefore at smaller barrier thicknesses. In particular, even in a perfect Fe/MgO/Fe crystal structure, one expects to measure no exponential increase in the TMR ratio with increasing barrier thickness. Sections VI and VII analyze and explain the reason for the saturation by means of the complex band structure of MgO.

V. TUNNELING STATES AND DECAY RATES

To understand the saturation of the TMR ratio for thick barriers, one has to identify which tunneling states in the two-dimensional Brillouin zone have the largest contribution to the current. Quite often the tunneling current is interpreted in terms of states at the $\bar{\Gamma}$ point ($\mathbf{k}_\parallel=0$) only. In real systems, however, the $\bar{\Gamma}$ point does not dominate the total current. This fact will be analyzed in the following for the Fe/MgO/Fe system. The annulus within the 2D Brillouin zone, in which the states are located which carry 90% of the total current, is determined for every system under consideration. To give an example, in Fig. 3 the $\mathbf{k}_\parallel$-resolved transmission and the corresponding annulus are shown for the symmetric junction in the P configuration with a barrier thickness of 10 MgO monolayers. The size of the annulus is presented in Fig. 4 for all junction geometries we considered and all barrier thicknesses by the inner and outer radius, $k_<$ and $k_>$, respectively. The annulus shrinks rapidly up to ten MgO layers and contracts further but much slower for all geometries.

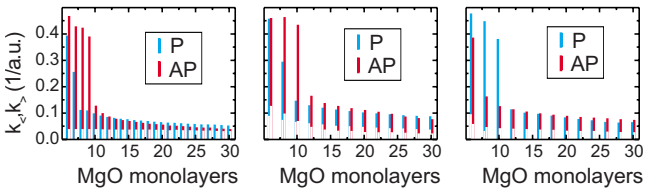

FIG. 4. (Color online) Annulus in $\mathbf{k}_\parallel$ space where the contribution to the complete transmission is 90% as a function of the barrier thickness for all geometries we considered: left, ideal; middle, symmetric; and right, asymmetric.

In agreement with other calculations,[32,33] the current is carried by a few states located in a small region of the $\mathbf{k}_\parallel$ space. The important fact is that for the ideal and asymmetric junction in the AP magnetic configuration, the annulus does not contain the $\bar{\Gamma}$ point and states next to it, whereas in the P configuration, the annulus in the $\mathbf{k}_\parallel$ space is nearly a circle around the $\bar{\Gamma}$ point. The reason for this behavior is the already mentioned symmetry selection of the MgO barrier. In the P configuration, the transport is dominated by the Δ_1-like states which have the lowest decay rate at the zone center whereas in the AP configuration the Δ_5-like states are important which have the lowest decay rate away from the zone center. Even at this point we want to mention that for thicker barriers the main contributions in the AP configuration are closer to the zone center where the Δ_5-like states already have a clearly larger decay rate than the Δ_1-like states. This implies that for thick barriers different states with respect to symmetry at the $\bar{\Gamma}$ point form the current in comparison to thin barriers. Before we prove this assumption, it is worth mentioning that in the symmetric geometry in both magnetic configurations the states close to $\mathbf{k}_\parallel=0$ do not contribute significantly to the current (compare Fig. 4, middle panel). This fact can be understood easily because the symmetry is only a necessary condition to obtain a high transmission probability. Even matching the symmetry some tunneling matrix elements can be small influenced by the interface structure.[34] In particular, the FeO at the interface leads to a reduction of the transmission probability at the $\bar{\Gamma}$ point for the P configuration. In the symmetric geometry, two FeO layers, one at each side, are present which leads to a strong reduction of the current contributions near the $\bar{\Gamma}$ point. However, in the asymmetric junction only one FeO layer is present and the transmission probability is large enough to contribute significantly around the $\bar{\Gamma}$ point in the *P* configuration of the asymmetric geometry.

To support our indication of different states dominating the current for thin and thick barriers, we want to analyze if the contributing states are Δ_1- or Δ_5-like states for thick barriers. For this purpose, the decay of $T_{\mathbf{k}_\parallel}(d)$ is analyzed for each $\mathbf{k}_\parallel$ point as a function of the barrier thickness d. The decay rate of the transmission probability is extracted by an exponential fit in the thickness range between 6 and 30 monolayers. Using this method, we calculated the maps of decay rates shown in Fig. 5. Thereby, we made this analysis for all three junction geometries, for all spin channels and for both magnetic configurations separately.

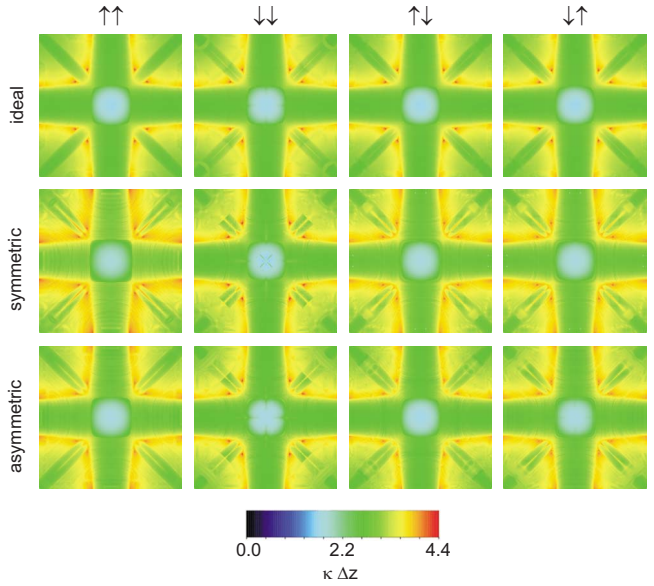

FIG. 5. (Color online) $\mathbf{k}_\parallel$-resolved decay rates determined from the $T_{\mathbf{k}_\parallel}(E_F)$ dependence on barrier thickness $d=6\cdots30$ monolayers for all geometries we considered: top, ideal; middle, symmetric; and bottom, asymmetric. The columns refer to the corresponding spin channels $\uparrow\uparrow$ and $\downarrow,\downarrow$ for the P and $\uparrow\downarrow$ and $\downarrow\uparrow$ for the AP configurations.

The comparison of these maps with the imaginary part of the complex wave vector of MgO in Fig. 1 shows that the dominating states for large barrier thickness are Δ_1-like states in all cases. This means that for the AP configuration for thin barriers the main contribution occurs from the Δ_5-like states of the leads but these contributions become negligible for thick barriers. Only the portions of the states which can couple to the Δ_1-like band of MgO contribute for large barrier thicknesses. Directly at the $\bar{\Gamma}$ point, the symmetry mismatch prohibits a contribution of Δ_1-like states in the AP configuration. This finding establishes that the significantly contributing tunneling states (see Fig. 4) have nearly the same decay rate for large barrier thickness independent on the spin channel, the magnetic configuration, and the interface structure. Consequently, the TMR ratio saturates for large barrier thicknesses since the exponential decay of *RA* is almost the same for the *P* and AP configuration. The asymptotic value of the TMR ratio is determined by the spin anisotropy of Δ_1-like states around the $\bar{\Gamma}$ point at the interface due to the matching conditions discussed above.

VI. OSCILLATION OF TUNNELING MAGNETORESISTANCE RATIO

Besides the saturation of the TMR ratio Yuasa *et al.*[9] and Matsumoto *et al.*[35] measured an oscillation of the TMR ratio as a function of the barrier thickness. In our calculation, we do not observe such an oscillating behavior (see Fig. 2). In general, an oscillating behavior of $T^{\sigma}_{\mathbf{k}_\parallel}$ depending on thickness d is caused by the real part of the complex wave vector of eigenstates in the band gap of MgO.[11] It was pointed out in Sec. VIII that all contributing states for large barrier thick-

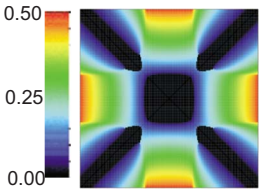

FIG. 6. (Color online) $\mathbf{k}_{\|}$-resolved real part of the complex wave vector in the MgO band gap of the band with the smallest imaginary part of the wave vector (Δ_1-like character) in units of $\pi/\Delta z$.

ness are Δ_1-like states. Therefore, only the real part of the wave vector shown in Fig. 6 of the corresponding complex band of MgO has to be analyzed. As shown in Fig. 4, the contributing states for large barrier thicknesses are located in a region around the $\bar{\Gamma}$ point where the real part of the wave vector of the corresponding complex band of MgO is zero. Therefore, no oscillations of the current density and resulting TMR ratios were obtained for all the junction geometries we considered. For this reason the TMR oscillations observed in Fe/MgO/Fe junctions[9,35] cannot be attributed to quantum size effects inside the ideal MgO tunneling barrier. Their occurrence is still under debate.

VII. CURRENT-VOLTAGE CHARACTERISTICS

The bias dependence for the junction with 4 MgO monolayers was already discussed in terms of the conductance and TMR ratio in Ref. 14. Following the above findings, one can expect significant changes of the contributing states concerning their positions in the Brillouin zone with increasing barrier thickness. Therefore, the important question arises, how characteristics features of the current-voltage characteristics change with increasing barrier thickness. It is not obvious that the features are conserved at different barrier thicknesses. In particular, it depends on the tunneling states that cause a specific feature. Therefore, we want to analyze what happens to the already discussed[14] fingerprints of the bias dependence for larger barrier thicknesses. The calculated bias dependence of the current density $I(V)$ is shown in Fig. 7 for all junction geometries we considered and for barrier thicknesses of 4, 8, and 12 monolayers. Surprisingly, the changes are very small, besides the expected strong exponential decrease of the current magnitude. The reader should notice the different scales of current. The striking features such as the sign reversal of the TMR in the symmetric geometry and the jump of the antiparallel current at a voltage of about 0.4 V in the asymmetric geometry remain even for thicker barriers. The origin of these features for a barrier of 4 MgO layers is discussed in detail in Ref. 14 and can be understood in terms of the $\mathbf{k}_{\|}$-resolved density of states at the interface and the tunneling matrix elements connecting both interfaces. In particular, the states which cause the main features have to be located close to the $\bar{\Gamma}$ point (see Fig. 4) and have to have Δ_1-like character (see Fig. 5) to persist for large barrier thicknesses. This is obviously the case for the features shown in Fig. 7, but this behavior cannot be generalized to other interfaces or lead materials. In particular, each specific

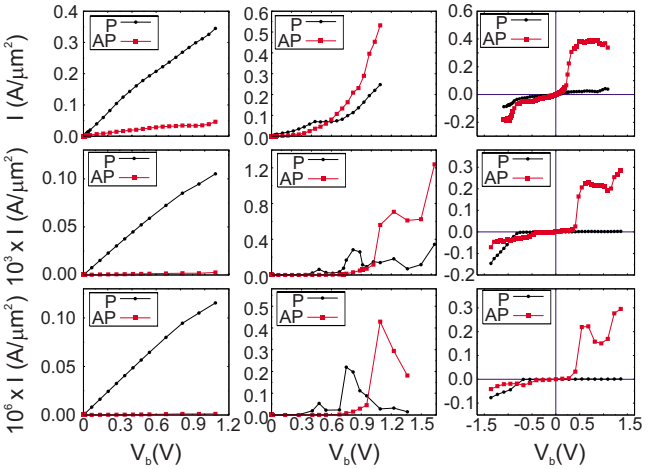

FIG. 7. (Color online) Bias dependence of the current density for three different barrier thicknesses and three junction geometries: top, 4 MgO layers (already published in Ref. 14); middle, 8 MgO layers; bottom, 12 MgO layers; left, ideal; middle, symmetric; and right, asymmetric

feature in a bias dependence has to be analyzed explicitly if it fulfills the mentioned conditions to persist for larger barrier thicknesses.

VIII. CONCLUSION

In conclusion, the current density of Fe/MgO/Fe tunnel junctions was calculated without adjustable parameters for different interface geometries as a function of the applied bias voltage and as a function of the barrier thickness. The zero-bias resistance shows an exponential increase with barrier thickness for all interface geometries but with slightly different slopes for small thicknesses. The experimentally observed saturation of the TMR ratio with barrier thickness can be reproduced in the coherent limit for the ideal crystalline structure without any defect scattering. The explanation of this saturation is that the fraction of Δ_1-like character of the states around the Brillouin-zone center dominates the current at large barrier thicknesses. Therefore, these states obey almost the same exponential decay and the resistances in P and AP configuration have nearly the same exponential increase. Characteristic features of the bias dependence of the TMR ratio are fingerprints of the coherent electronic structure and are stable as a function of barrier thickness for the geometries we considered. However, there is no general argument whether a specific feature is conserved also for larger barrier thicknesses. Furthermore, the experimentally observed oscillations of the TMR ratio with barrier thickness[9,35] are not an intrinsic quantum size effect of the ideal crystalline Fe/MgO/Fe tunnel junction since the real part of the complex wave vector of the MgO band-gap states is zero for the relevant states.

ACKNOWLEDGMENTS

We thank M. D. Stiles for fruitful discussions. Financial support by the DFG (FG 404) is kindly acknowledged.

*christian.heiliger@physik.uni-halle.de

[1] S. S. P. Parkin, N. More, and K. P. Roche, Phys. Rev. Lett. **64**, 2304 (1990).
[2] M. N. Baibich, J. M. Broto, A. Fert, F. Nguyen Van Dau, F. Petroff, P. Etienne, G. Creuzet, A. Friederich, and J. Chazelas, Phys. Rev. Lett. **61**, 2472 (1988).
[3] G. Binasch, P. Grünberg, F. Saurenbach, and W. Zinn, Phys. Rev. B **39**, 4828 (1989).
[4] M. D. Stiles, Phys. Rev. B **48**, 7238 (1993).
[5] P. Bruno and C. Chappert, Phys. Rev. Lett. **67**, 1602 (1991).
[6] M. van Schilfgaarde and W. A. Harrison, Phys. Rev. Lett. **71**, 3870 (1993).
[7] J. S. Moodera, L. R. Kinder, T. M. Wong, and R. Meservey, Phys. Rev. Lett. **74**, 3273 (1995).
[8] T. Miyazaki and N. Tezuka, J. Magn. Magn. Mater. **139**, L231 (1995).
[9] S. Yuasa, T. Nagahama, A. Fukushima, Y. Suzuki, and K. Ando, Nat. Mater. **3**, 868 (2004).
[10] C. Tiusan, J. Faure-Vincent, C. Bellouard, M. Hehn, E. Jouguelet, and A. Schuhl, Phys. Rev. Lett. **93**, 106602 (2004).
[11] W. H. Butler, X. G. Zhang, T. C. Schulthess, and J. M. MacLaren, Phys. Rev. B **63**, 054416 (2001).
[12] C. Zhang, X. G. Zhang, P. S. Krstić, H. P. Cheng, W. H. Butler, and J. M. MacLaren, Phys. Rev. B **69**, 134406 (2004).
[13] C. Heiliger, P. Zahn, B. Y. Yavorsky, and I. Mertig, Phys. Rev. B **72**, 180406(R) (2005).
[14] C. Heiliger, P. Zahn, B. Y. Yavorsky, and I. Mertig, Phys. Rev. B **73**, 214441 (2006).
[15] P. LeClair, H. J. M. Swagten, J. T. Kohlhepp, R. J. M. van de Veerdonk, and W. J. M. de Jonge, Phys. Rev. Lett. **84**, 2933 (2000).
[16] P. LeClair, J. T. Kohlhepp, H. J. M. Swagten, and W. J. M. de Jonge, Phys. Rev. Lett. **86**, 1066 (2001).
[17] J. M. De Teresa, A. Barthélémy, A. Fert, J. P. Contour, R. Lyonnet, F. Montaigne, P. Seneor, and A. Vaurès, Phys. Rev. Lett. **82**, 4288 (1999).
[18] J. Mathon and A. Umerski, Phys. Rev. B **74**, 140404(R) (2006).
[19] J. Velev, K. Belashchenko, S. Jaswal, and E. Tsymbal, Appl. Phys. Lett. **90**, 072502 (2007).
[20] H. L. Meyerheim, R. Popescu, J. Kirschner, N. Jedrecy, M. Sauvage-Simkin, B. Heinrich, and R. Pinchaux, Phys. Rev. Lett. **87**, 076102 (2001).
[21] C. Tusche, H. L. Meyerheim, N. Jedrecy, G. Renaud, A. Ernst, J. Henk, P. Bruno, and J. Kirschner, Phys. Rev. Lett. **95**, 176101 (2005).
[22] C. Heiliger, P. Zahn, and I. Mertig, J. Magn. Magn. Mater. **316**, 478 (2007).
[23] R. Zeller, P. H. Dederichs, B. Újfalussy, L. Szunyogh, and P. Weinberger, Phys. Rev. B **52**, 8807 (1995).
[24] N. Papanikolaou, R. Zeller, and P. Dederichs, J. Phys.: Condens. Matter **14**, 2799 (2002).
[25] R. Landauer, Z. Phys. B: Condens. Matter **68**, 217 (1987).
[26] H. U. Baranger and A. D. Stone, Phys. Rev. B **40**, 8169 (1989).
[27] N. Mott, Adv. Phys. **13**, 325 (1964).
[28] P. Mavropoulos, N. Papanikolaou, and P. H. Dederichs, Phys. Rev. B **69**, 125104 (2004).
[29] D. Pettifor, Commun. Phys. (London) **1**, 141 (1976).
[30] D. Pettifor and C. Varma, J. Phys. C **12**, L253 (1979).
[31] P. Mavropoulos, N. Papanikolaou, and P. H. Dederichs, Phys. Rev. Lett. **85**, 1088 (2000).
[32] J. Mathon and A. Umerski, Phys. Rev. B **63**, 220403(R) (2001).
[33] J. P. Velev, K. D. Belashchenko, D. A. Stewart, M. van Schilfgaarde, S. S. Jaswal, and E. Y. Tsymbal, Phys. Rev. Lett. **95**, 216601 (2005).
[34] I. I. Mazin, Europhys. Lett. **55**, 404 (2001).
[35] R. Matsumoto, A. Fukushima, T. Nagahama, Y. Suzuki, K. Ando, and S. Yuasa, Appl. Phys. Lett. **90**, 252506 (2007).